Mapping of the Multi-risk Analysis for the Cultural Heritage of Sardinia from the Pre-Nuragic and Nuragic Periods: Initial Results of the RETURN Project

Enrica Vecchi(✉), Marco Cigagna, Donatella Rita Fiorino, Battista Grosso, Elisa Pilia, Francesco Pinna, and Giuseppina Vacca

Department of Civil and Environmental Engineering and Architecture (DICAAR), University of Cagliari, 09123 Cagliari, Italy
enrica.vecchi@unica.it

Abstract. Sardinia's cultural heritage features unique prehistoric structures from the pre-Nuragic and Nuragic periods (5th–6th centuries BC). These include Nuraghi, giants' tombs, sanctuaries, Domus de Janas, dolmens, menhirs, and megalithic circles. Given their complexity and the increasing threat from climate change, a comprehensive database and spatial mapping system are vital for their preservation. This study presents initial findings from Project RETURN (multi-Risk sciEnce for resilienT commUnities undeR a changiNg climate), which focuses on systematic risk analysis for Sardinia's cultural heritage. A unified database was created using public inventories, standardizing data and assigning simplified attributes based on monument dimensions (e.g., tall, subterranean). GIS tools enabled precise georeferencing, material characterization (via lithological maps), and automatic exclusion of sediment categories based on proximity and area size. Each structure was assigned vulnerability levels (Very Low to Very High) based on geometry and construction material, in relation to four hazard types: hydraulic, hydrogeological, seismic, and wildfire. Hazard data from regional sources were normalized and matched to monument locations. This allowed for the generation of both individual and multi-risk maps using a consistent five-level classification system. The resulting spatial analyses provide valuable insights into the exposure and resilience of heritage sites across Sardinia. These findings support informed decision-making for conservation efforts, with risk visualizations available at both site and regional scales.

Keywords: Multi-risk · cultural heritage · GIS · mapping

1 Introduction

Sardinia's cultural heritage is marked by unique structures that date back to the pre-Nuragic (5th to 3rd millennium BC) and Nuragic (18th to 6th centuries BC) periods, spanning the Neolithic to the Early Iron Age [1–3]. Indeed, this era saw the arising of various structures of significant historical and archaeological value. Notable ancient

© The Author(s), under exclusive license to Springer Nature Switzerland AG 2026
O. Gervasi et al. (Eds.): ICCSA 2025, LNCS 15898, pp. 327–344, 2026.
https://doi.org/10.1007/978-3-031-97657-5_20

megalithic edifices characteristic of the island include Nuraghi, giant's tombs, sanctuaries, Domus de Janas, caves, shelters, menhirs, dolmens, and megalithic circles. Given the uniqueness, complexity, and diversity of these constructions, creating a comprehensive and updated database along with detailed mapping of each site is essential for monitoring and preserving this heritage. This task is especially critical in light of the complex territorial context, where environmental phenomena are exacerbated by climate change. In this regard, Geographic Information Systems (GIS) serve as crucial tools, allowing for the integration of data from various sources, accurate site georeferencing, and the combination of specific attributes, in addition to enabling a wide range of spatial analyses to derive further insights [4–8].

Although there is an increasing amount of research on the vulnerability of cultural heritage to environmental hazards, most existing studies tend to focus on structures from the medieval to modern periods. These studies often assess risks at broader geographic scales, such as urban areas or landscape units [9, 10]. In contrast, prehistoric monuments, particularly those in Sardinia, represent complex and context-specific subjects that require further in-depth investigation. Notably, there is currently no comprehensive official database that includes the island's prehistoric structures, which differ significantly in both architecture and environmental context from those found in other regions of Italy [11]. Furthermore, Sardinia faces unique hazard challenges, such as uneven seismic activity, specific hydrogeological risks, and an increasing frequency of wildfires, all of which complicate heritage management efforts [12–14].

This study presents the initial findings from Project RETURN (multi-Risk sciEnce for resilienT commUnities undeR a changiNg climate), which focuses on the systematic mapping of multi-risk analyses concerning Sardinian cultural heritage from the Nuragic and pre-Nuragic periods. In particular, the GIS environment supported all phases of the analysis, starting from the finalization of the database. Official maps concerning hydraulic, hydrogeological (referred to as "landslides"), and wildfires hazards were used, whereas a uniform value was applied for seismic hazard across the region. The vulnerability of structures based on their dimensions and geometry was assessed and is reported in this paper for the sake of completeness, even though a full explanation is beyond the scope of this paper. A detailed spatial analysis was conducted to determine construction materials based on a proximity principle applied to the official regional lithologic map. Finally, by properly defining the database, automated GIS and Python-based procedures were employed to associate vulnerabilities and hazard values with each considered monument, allowing for the retrieval of respective risk and multi-risk values [15–17]. As a primary result, the multi-risk analysis adopted a maximum approach, providing insights into possible critical situations related to specific monuments or municipality that would require more careful management.

The novel contribution of this research lies in its monument-specific approach, which integrates hazard exposure, structural characteristics, and inferred construction materials into a unified, replicable GIS-based framework. This enables the generation of risk maps at both micro (individual monument) and macro (regional) scales—offering a valuable decision-support tool for cultural heritage management, maintenance, and adaptation planning. By addressing data gaps and developing site-specific assessments in a region lacking centralized records, this work sets a foundation for proactive heritage risk governance in Sardinia and offers a scalable methodology for other contexts.

2 Materials

2.1 Database and Building Typologies

The primary objective of this study was to create a unified database of the cultural heritage sites in the Sardinia region, specifically those from the pre-Nuragic period (5th to 3rd millennium BC) and the Nuragic period (18th to 6th centuries BC). In particular, the final database was designed for GIS use and formatted as a vector dataset in shapefile format. To achieve this, two publicly available inventories were utilized. The first was obtained from "SardegnArcheologica," an initiative focused on cataloging and georeferencing Sardinia's archaeological sites, with a particular emphasis on Nuraghi [18]. This open-access database is available for both online browsing and downloading and includes a significant number of monuments, such as Nuraghi and Giants' tombs, reflecting the extensive distribution of these structures across Sardinia. The second data source, "Nurnet – La rete dei Nuraghi," stems from a participatory initiative aimed at documenting and promoting Sardinia's Nuragic and pre-Nuragic cultural heritage [19]. This inventory is accessible through a dedicated Geoportal, a web-based platform that allows interactive access to data. Therefore, expert and non-expert users—such as citizens, tourists, associations, and institutions—can visualize and browse site information and also directly contribute by adding or updating data, including textual descriptions and photographs. Because of this, the data in this inventory is continually updated and undergoes a reviewing phase by experts in the field, which should be taken into account when using it.

For this study, we focused on different building typologies covered by both databases. To avoid duplication, we first extracted the chosen typologies from the SardegnArcheologica inventory and used the Nurnet database to complete the categories that were not present in the first source, as shown in Table 1.

After downloading the two datasets in shapefile format, we first selected the chosen building typologies from the data sources, ensuring a common format was applied and essential information was simplified. The combination of these two data sources resulted in a total of 7,335 monuments located throughout Sardinia. Figure 1a displays the Sardinian map with the completed regional database, while the pie chart in Fig. 1b illustrates the percentage of coverage of the various types of structures.

Table 1. Building typologies retrieved from the two regional public inventories of archaeological monuments.

SardegnArcheologica	Nurnet
Nuraghi	Domus de Janas
Giants' tombs	Menhir
Springs	Dolmen
Sacred wells	Caves and shelters
Sanctuaries	Megalithic circles

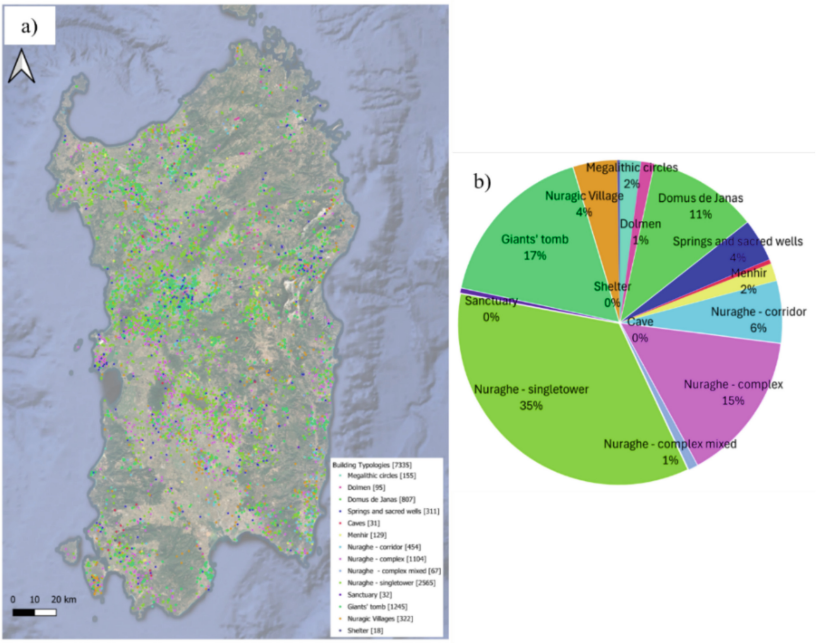

Fig. 1. Completed regional database with the building typologies (a); pie chart showing typology percentages (b).

In parallel, the building typologies were characterized with specific attributes based on their geometry and dimensions, considering the overall proportions of each type of structure (tall, equidimensional, small, subterranean, wide). For the sake of simplicity, a numerical ID was assigned to each typology, as listed in Table 2, which also provides information regarding historical periods.

2.2 Materials Analysis

In addition to the dimensional characteristics of each structure, we focused on the construction materials, which are crucial for assessing the monuments' vulnerability to

Table 2. Classification of the selected building typologies in terms of geometry and historical period.

ID	Building Typology	Geometry	Period
5.1	Nuraghe – corridor	Equidimensional (B)	1700–1350 B.C., Middle Bronze Age
5.2	Nuraghe – singletower	Equidimensional (B)	1500–1350 B.C
5.3	Nuraghe - complex	Equidimensional (B)	
5.4	Giants' tomb	Wide (E)	Bronze Age
5.5	Sacred weels	Subterranean (D)	Bronze Age, early Iron Age
5.6	Domus de Janas	Subterranean (D)	1800–1600 B.C., Middle Neolithic
5.7	Cave	Subterranean (D)	From 5th to the end of the 3rd millennium B.C
5.8	Shelter	Small (C)	From 5th to the end of the 3rd millennium B.C
5.9	Menhir	Tall (A)	From Neolithic to Copper Age
5.10	Dolmen	Tall (A)	From Neolithic to Copper Age
5.11	Megalithic circles	Tall (A)	Middle Neolithic
5.12	Sanctuary	Wide (E)	
5.13	Nuragic Village	Wide (E)	1350 B.C. – 950 B.C

various hazards. However, this information is not available for most of the mapped sites, with only a few significant ones from cultural and touristic perspectives providing material details. Consequently, some simplifying assumptions were necessary during this step of the analysis. Given the complexity of the territory and the significant topographical variations - even among nearby areas - it seemed unlikely that non-local materials would be used for construction. Therefore, we deduced the construction materials from the in-situ lithology. This assumption is also supported by real cases that confirm the use of local materials for constructions, especially considering the weight of the megalithic blocks. Notable examples include the famous Su Nuraxi of Barumini, Santu Antine, and Losa, which suggest that transporting massive stones over long distances would be impractical, leading to a preference for locally abundant stones.

Despite the supporting reasons for using lithological maps, this approach has some limitations. Indeed, while these maps can provide general geological information, they may not accurately reflect localized material selections. In certain cases, short-range transportation of materials might have been practical or necessary due to specific properties or symbolic significance. Furthermore, some changes that occurred after deposition could lead to discrepancies between the original materials and the current lithological context. Future steps will aim to validate this analysis through field surveys, archaeological reports, or the integration of other data sources to enhance reliability.

The construction materials for each monument was determined though a spatial analysis conducted using QGIS software, based on the official regional lithological map shown in Fig. 2 [20]. For clarity, the map's legend in Fig. 2 presents the classifications with associated alphanumeric labels corresponding to the different lithologies; additional information can be obtained by consulting the original data source.

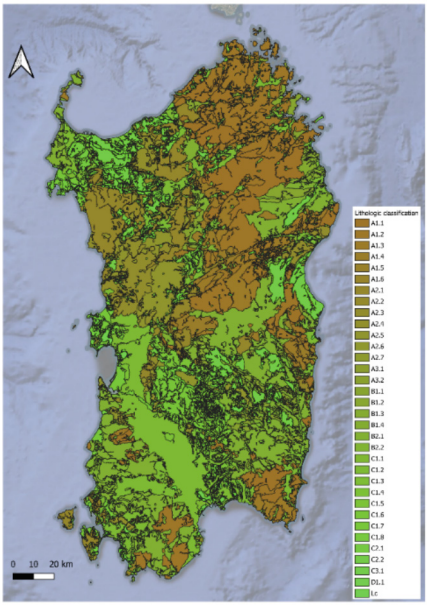

Fig. 2. Lithologic map of Sardinia [20].

The official classification of lithologic materials includes 34 detailed categories, covering a variety of rock types as well as other classifications such as lakes and anthropogenic artifacts. Based on the aforementioned assumptions, it was necessary to exclude categories that do not represent viable construction materials, specifically sedimentary rocks, lakes, and anthropogenic artifacts.

After sampling the lithologic map at the locations of the monuments and assigning the corresponding classes to each, a procedure using GIS and Python was implemented to address cases related to the excluded classes. For monuments located within polygons associated with the excluded categories, the algorithm searches the neighboring polygons to identify the most probable lithology based on a detailed proximity principle. In particular, the analysis focused on the following parameters:

- dist_b: Shortest distance between the monument and the polygon's boundary
- area: Area of the polygon
- dist_c: Distance between the monument and the polygon's centroid

For each neighboring polygon i, different weights were assigned as follows:

$$w_{i,dist_b} = \frac{1}{dist_b_i} \tag{1}$$

$$w_{i,area} = \frac{area_i}{\sum_i^n area_i} \tag{2}$$

$$w_{i,dist_c} = \frac{1}{dist_c_i} \tag{3}$$

where n represents the total number of neighboring polygons.

The final score was calculated as:

$$S_i = w_{i,dist_b}^{\alpha} \cdot w_{i,area}^{\beta} \cdot w_{i,dist_c}^{\gamma} \tag{4}$$

In Eq. (4), α and β were set equal to 1, while γ was assigned a value of 2. The distances from the polygon's boundary and the area of the polygon were considered linearly, ensuring that polygons closer to the monument were preferred and larger polygons had a proportional impact without dominating the score. The distance from the polygon's centroid was given a quadratic weight, making it the most significant factor, and prioritizing it over the other two factors. Indeed, given the complexity and irregular shapes of the lithology polygons, a closer centroid suggests that the majority of the polygon is distributed near or around the monument. This weighting methodology helps to filter out polygons with misleading thin extensions or elongated parts that might otherwise appear relevant due to proximity based on boundary distance. Such polygons reaching close to the monument, having a small boundary distance, could falsely suggest a strong relevance. Moreover, the resulting ranking is more robust since the score decreases more sharply as the centroid distance increases compared to the other parameters (α and β). This ensures that only polygons with most of their mass near the monument remain highly ranked. By using this metric of proximity, we achieved a better understanding of the polygon's actual location and we were able to identify the most likely construction material, corresponding to the lithology with the highest score.

Next, the appropriate valid lithologic class was assigned to each monument, grouping them into macro-categories as shown in Table 3 to simplify the analysis. This clustering not only simplifies the classification process but also supports the underlying hypothesis of the spatial analysis used to derive the construction materials, as it averages the initial detailed categories.

Table 3. Grouped materials categories.

Official lithologic class	New class
A1.1, A1.2, A1.3, A1.4, A1.5, A1.6	Granites
A2.1, A2.2, A2.4	Trachytes auctorum
A2.3, A.2.5, A.2.6, A2.7	Alkaline vulcalites (basalts)
B1.1, B1.2, B1.3, B1.4, B2.1	Metamorphites
B2.2, C2.1, C2.2	Carbonates

The spatial analysis results for defining the construction material are illustrated in Fig. 3a. Figure 3b presents a pie chart that shows the percentage distribution of each material classification.

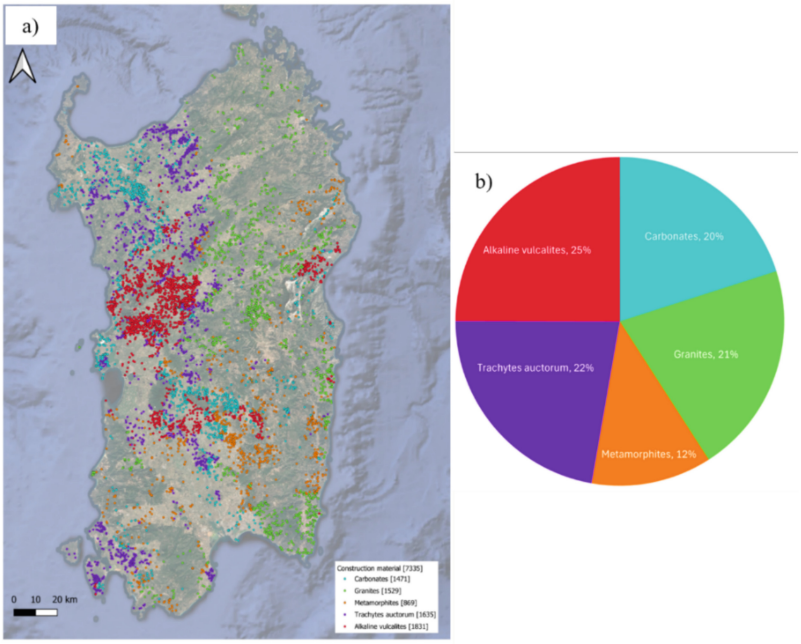

Fig. 3. Completed regional database with the construction materials (a); pie chart depicting materials percentages (b).

3 Methods

3.1 Vulnerability Analysis

Based on the previously established classifications regarding geometry and construction materials, two types of vulnerability were defined, which vary depending on the related hazard *i* (Hydraulic - *h*, Landslides - *l*, Wildfire - *w*, Seismic - *s*). These vulnerabilities are defined as follows:

- $V_{geom,i}$: Vulnerability related to geometry
- $V_{mat,i}$: Vulnerability related to construction material

To achieve this, specific matrices were developed to assess the level of vulnerability based on both geometric and material characteristics. In particular, each was classified into 5 levels: Very Low (VL), Low (L), Medium (M), High (H), and Very High (VH), corresponding to numerical values ranging from 1 (VL) to 5 (VH). An example of the vulnerability matrix related to hydraulic hazard is presented in Table 4, while the complete set of matrixes can be found in the Appendix. It is important to note that the detailed considerations leading to the construction of the vulnerability matrices are beyond the scope of this paper, which focuses instead on spatial analysis and mapping.

Table 4. Example of vulnerability matrix related to hydraulic hazard.

Building ID	$V_{geom,h}$	Material	$V_{mat,h}$
5.1	2	Granites	1
5.2	2	Trachytes auctorum	1
5.3	2	Alkaline vulcalites	2
5.4	3	Metamorphites	3
5.5	4	Carbonates	4
5.6	4		
5.7	4		
5.8	3		
5.9	2		
5.10	2		
5.11	2		
5.12	3		

In this phase, proper codification of the database was essential to automatically associate each monument with its related vulnerabilities, depending on the building type and construction material used. As a result, the database was completed with eight additional fields, representing two types of vulnerability for four considered hazards: $V_{geom,h}$; $V_{mat,h}$; $V_{geom,l}$; $V_{mat,l}$; $V_{geom,w}$; $V_{mat,w}$; $V_{geom,s}$; $V_{mat,s}$.

3.2 Hazards

The hazard analysis was based on the official maps sourced from the PAI (Piano Stralcio per l'Assetto Idrogeologico) and the Geoportal of the Sardinia region [21–23]. Specifically, maps for the hydraulic and hydrogeological ("landslides") hazards were retrieved from the first source, while the second was used to download the wildfire map, given its specificity for the Sardinia region, which particularly suffers from this issue [24, 25]. Conversely, since Sardinia is known to be particularly stable from a seismic point of view [26–28], no seismic hazard map was employed, and a fixed hazard value was applied instead, which will be further discussed. For more detailed information, please consult the official maps and their classifications.

As a preliminary step, the official hazard maps were resampled on the monuments' positions, generating additional fields that contained the corresponding official hazard classes. Subsequently, the official categories were simplified, providing a numeric and unified classification divided into five classes with equivalent meanings. The adopted approach is detailed in Table 5, which outlines the official hazard classes alongside their corresponding values for our analysis. Notably, for the wildfire hazard, the two classifications are equivalent since the official maps already employed a numeric classification. Here, the lower class is absent, denoting the region's inherent fire exposure. As mentioned earlier, a constant value of $H_s = 1$ was assigned to the seismic hazard to indicate the low seismicity in Sardinia while preventing a total underestimation of the issue (without using class 0).

Table 5. Adopted classification on the hazard classes, starting from the official categories.

Hydraulic *h*		Landslides *l*		Wildfires *w*		Seismic *s*
official	**new**	**official**	**new**	**official**	**new**	Constant value $H_s = 1$
Hi0	0	Hg0	0	/	/	
Hi1	1	Hg1	1	1	1	
Hi2	2	Hg2	2	2	2	
Hi3	3	Hg3	3	3	3	
Hi4	4	Hg4	4	4	4	
No value	0	No value	0	/	/	

Following this step, four new fields were associated to each monument: H_h; H_l; H_w; H_s.

4 Results

Having completed the monuments' database with the associated classes of vulnerabilities and hazards enabled the assessment of the related risks. In general, the risk can be calculated as follows [29, 30]:

$$R = V \cdot H \tag{5}$$

where V is the vulnerability and H is the associated hazard value.

The following paragraphs detail the workflow applied to create regional risk maps, focusing on both individual risk levels and multi-risk combinations, always adhering to the mentioned five-levels classification system.

4.1 Risk Analysis

For each hazard *i* (hydraulic, landslides, wildfires, and seismic) we calculated the associated risk value R_i as:

$$R_i = H_i \cdot V_{geom,i} \cdot V_{mat,i} \tag{6}$$

Subsequently, normalization was applied to adjust the final values to the five-level scale, considering the minimum and maximum possible risk values $R_{i,min}$ and $R_{i,max}$:

$$R_{i,min} = 0 \tag{7}$$

$$R_{i,max} = H_{i,max} \cdot V_{geom,i,max} \cdot V_{mat,i,max} = 4 \cdot 5 \cdot 5 = 100 \tag{8}$$

At this point, each risk value was reclassified according to the criteria outlined in Table 6, which divides values from 1 to 100 into 5 distinct risk classes.

Table 6. Risk classification according to the 5-level scale.

0-20	20-40	40-60	60-80	80-100
1	2	3	4	5
VL	L	M	H	VH

For each risk, we produced a comprehensive map reporting risk values associated with each considered monument (Figs. 4 and 5).

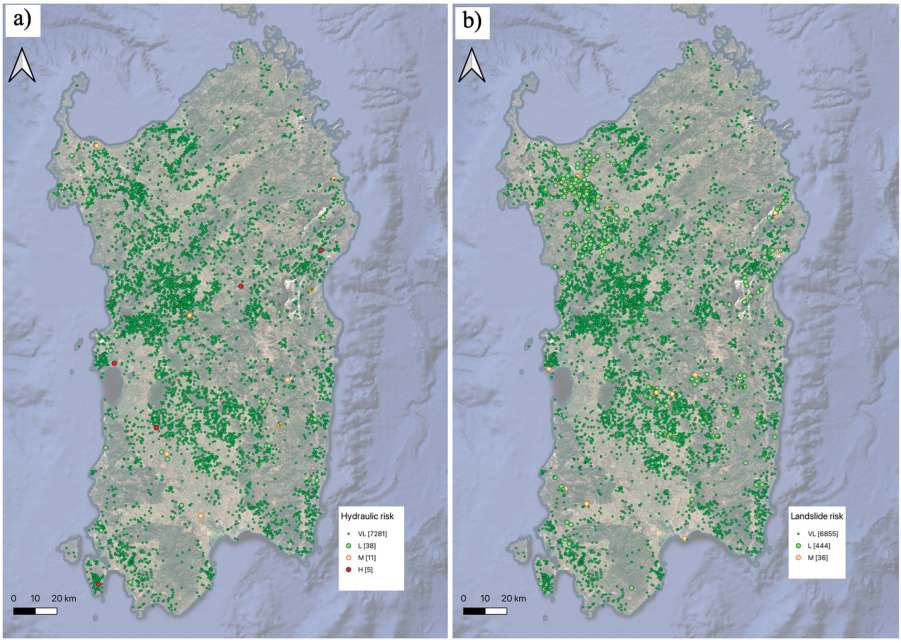

Fig. 4. Risk maps for hydraulic (a) and landslides risks (b).

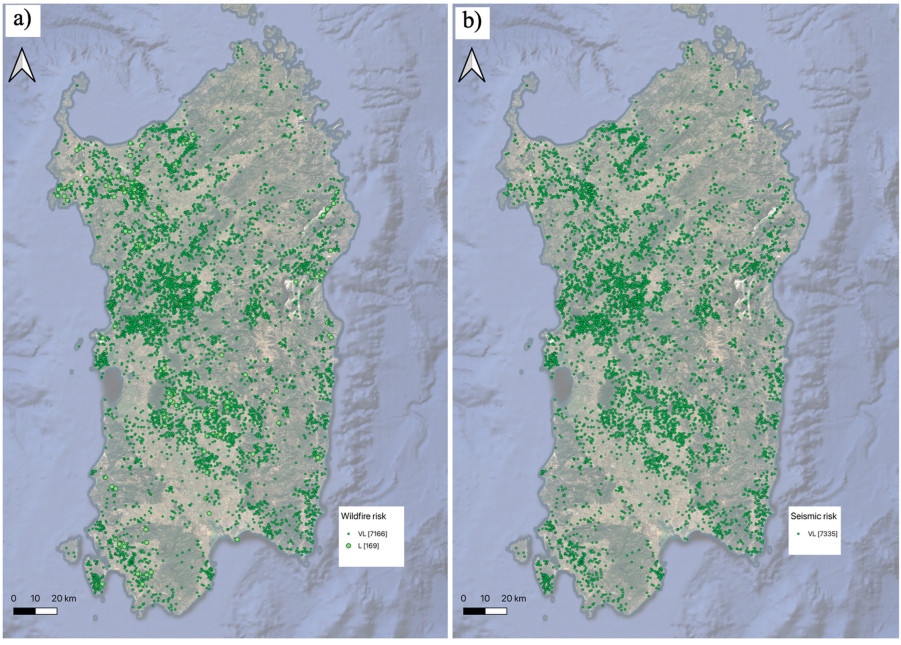

Fig. 5. Risk maps for wildfires (a) and seismic risks (b).

4.2 Multi-Risk Analysis

Monuments

For each monument we had the previously computed risk values, R_i, associated with each individual hazard. We then assigned the multi-risk value to each monument by taking the maximum of the individual risk values:

$$MR_{monument} = \max(R_h, R_l, R_w, R_s) \tag{9}$$

Therefore, the obtained MR values were already aligned to the 5-level scale classification described in Table 6. The selected approach adopts a conservative estimation that describes the worst-case scenario while also assuming no interaction between the considered hazards. Figure 6 displays the multi-risk map for all the selected monuments (a) along with a pie chart illustrating the percentage of each risk class. This map shows the prevalence of low-risk classes, particularly focusing on those that belong to the very low category. These values, despite some high hazard levels across the region, especially concerning the wildfire risk, were expected due to the low associated vulnerabilities related to strong rock or subterranean structures.

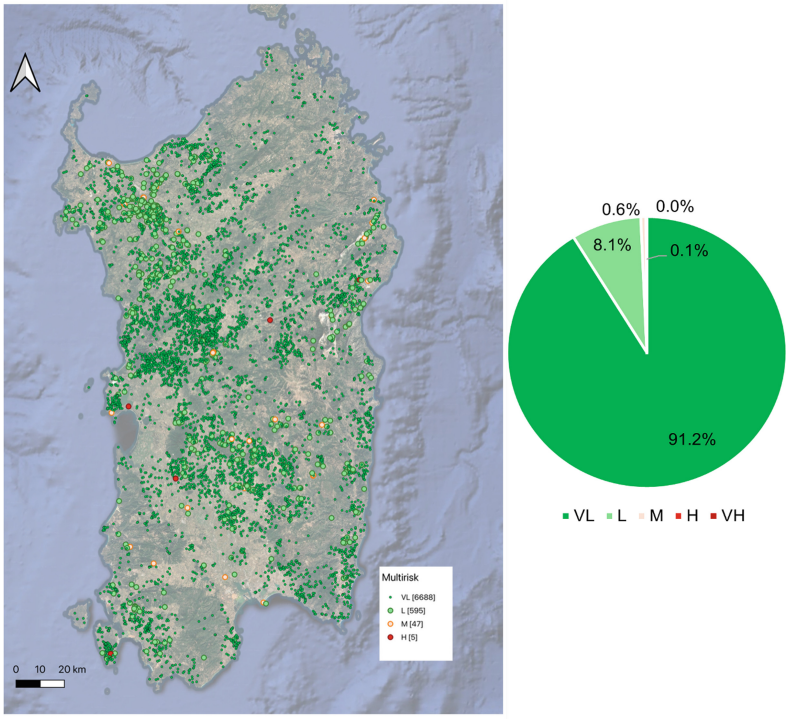

Fig. 6. Multi-risk map of the selected monuments (a); pie chart of classes' percentages (b).

Municipalities

For each municipality, we considered the number n of related monuments, and we assigned the corresponding multi-risk value as follows:

$$MR_{municipality} = \max(MR_{monuments}) \tag{10}$$

This conservative approach aims at highlighting critical situations in municipalities where at least one element is in a critical condition, thereby suggesting the need for greater caution in managing these areas. Figure 7 presents the multi-risk map at the municipality level (a) and a pie chart showing the percentage of each class.

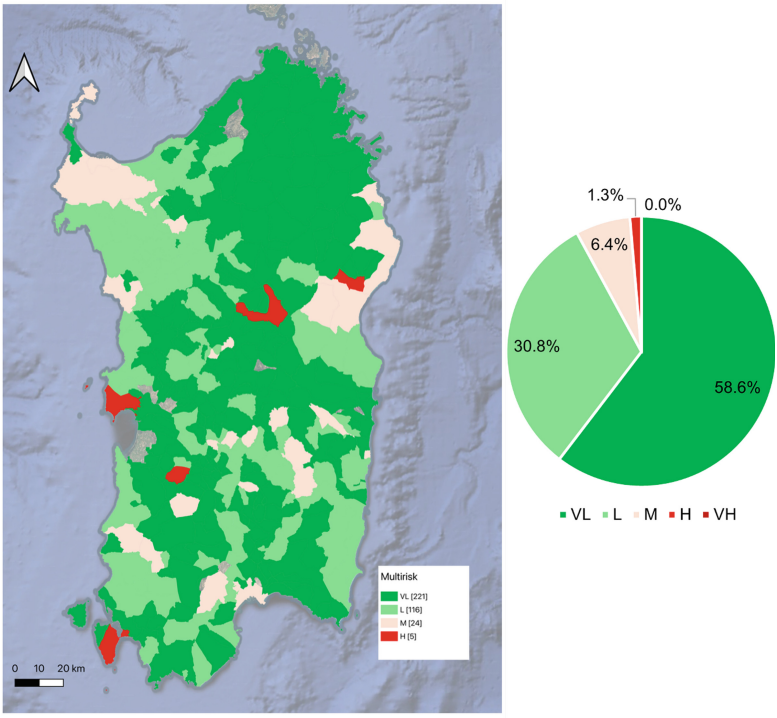

Fig. 7. Multi-risk map of Sardinia's municipalities (a); pie chart of classes' percentages (b).

5 Discussion and Conclusions

This paper aims to establish the foundation for a comprehensive database that documents cultural heritage sites from the pre-Nuragic and Nuragic periods in Sardinia. The first outcome highlights the wide number and dense distribution of these unique constructions, with over 7,000 features spread across the region. The distribution and characterization of these sites are increasingly significant for both researchers and the general public,

as they hold considerable historical and archaeological value for the region. In this context, effective management and preservation are crucial to promote accessibility and enhance the understanding of Sardinia's rich archaeological heritage, thereby fostering greater public engagement with the island's cultural landscape. This detailed database was utilized to conduct automated spatial analyses and procedures to assess the exposure of these monuments to various risks, including hydraulic, hydrogeological, wildfire, and seismic threats.

The reported risk analysis describes a stable situation for most of the considered monuments in Sardinia. Specifically, the percentages for the very low (VL) risk class range from 93% for landslides to 100% for seismic risks. In particular, the high percentage relating to seismic risk was completely expected, given the typical stability of the Sardinia region. This scenario is also reflected by the multi-risk analysis, besides applying a conservative approach by assigning the maximum single risks as multi-risk value. In this analysis, the 91% of the monuments fall into the very low class, while 8% are classified as low. The more critical classes (high and very high) show percentages close to zero.

The multi-risk analysis was also conducted at the municipality level, in order to highlight possible critical situations that may require more careful management, potentially leading to increased administrative costs. This computation, which also follows a conservative approach by assigning the highest risk among the local monuments to the entire municipality area, describes a slightly more critical situation compared to the analysis at the monument level. Due to the previous results, none of the municipalities falls into the very high risk category, while 1.3% and 6.4% belong are classified as high and medium risk, respectively. This kind of computation mainly resulted in a shift from the very low to the low risk class, with approximately 59% in the very low class and 31% in the low class.

The maximum risk approach selects the highest individual risk among multiple hazards to represent overall risk. This method simplifies decision-making by focusing on the most severe potential impact and can be used in certain multi-hazard assessments. For example, the study by Martín-Raya et al. (2024) employs a quasi-maximum approach, analyzing each hazard separately and identifying areas where multiple hazards overlap [31]. However, since their study examines the entire La Palma region, it addresses a different challenge than our analysis, which focuses on the monument level. Kappes et al. (2012) discuss the practical applications of various multi-risk analyses, particularly in disaster risk management, urban planning, and emergency response [32]. They highlight that all existing methods have limitations, indicating that the maximization method might be useful in some cases but could oversimplify complex interactions and dependencies among hazards.

In this context, the primary objective of our multi-risk assessment is to provide a valuable tool for the initial planning of structure management and preservation. The proposed assessment prioritizes the most severe risks, thereby enhancing resilience against the most damaging potential events. The results can be effectively visualized at the monument level using colour scales based on the final risk value. Alternatively, they can be aggregated at a macro-aerial scale to quickly understanding the risk levels across the Sardinia region. This study's insights establish a foundation for developing monitoring

parameters for cultural heritage. Additionally, further research will focus on implementing more advanced multi-risk analyses that account for interactions and potential cumulative effects.

Funding. This research was funded by PNRR - PE3 - RETURN - multi-Risk sciEnce for resilienT commUnities undeR a changiNg climate (CODICE MUR PE0000005).

Appendix

See Tables 7, 8 and 9.

Table 7. Vulnerability matrix for the landslides hazard.

Building ID	$V_{geom,l}$	Material	$V_{mat,l}$
5.1	2	Granites	2
5.2	2	Trachytes auctorum	2
5.3	2	Alkaline vulcalites	3
5.7	3		
5.8	2		
5.9	4		
5.10	4		
5.11	4		
5.12	2		

Table 8. Vulnerability matrix for the wildfires hazard.

Building ID	$V_{geom,l}$	Material	$V_{mat,l}$
5.1	2	Granites	1
5.2	2	Trachytes auctorum	2
5.3	2	Alkaline vulcalites	1
5.4	2	Metamorphites	2
5.5	1	Carbonates	3
5.6	1		
5.7	1		
5.8	2		
5.9	3		
5.10	3		
5.11	3		
5.12	2		

Table 9. Vulnerability matrix for the seismic hazard.

Building ID	$V_{geom,s}$	Material	$V_{mat,s}$
5.1	2	Granites	2
5.2	2	Trachytes auctorum	1
5.3	2	Alkaline vulcalites	3
5.4	2	Metamorphites	3
5.5	3	Carbonates	4
5.6	3		
5.7	3		
5.8	2		
5.9	4		
5.10	4		
5.11	4		
5.12	2		

References

1. UNESCO World Heritage Centre. Art and Architecture in the Prehistory of Sardinia. The domus de janas. https://whc.unesco.org/en/tentativelists/6523/. Last accessed 01 March 2025
2. Schirru, D., Perra, M., Holt, E., Lai, L.: A reassessment of the relative chronology of the Sardinian Middle Bronze Age: Results from the excavations of Nuraghe Sa Conca 'e sa Cresia, Siddi, Sardinia (2023)
3. Cicilloni, R., Cabras, M., Porcedda, F., Cámara Serrano, J.A.: Protohistoric landscapes in Sardinia (Italy): Territorial control and exploitation of natural resources in the Middle and Late Bronze Ages. Cuadernos de Prehistoria y Arqueología **31**, 19–38 (2021)
4. Longley, P.A., Goodchild, M.F., Maguire, D.J., Rhind, D.W.: Geographic information science and systems. John Wiley & Sons, Hoboken (2015)
5. O'sullivan, D., Unwin, D.: Geographic information analysis. John Wiley & Sons, Hoboken (2002)
6. Rocheford, M.K.: GIS for Science: Applying Mapping and Spatial Analytics. Photogramm. Eng. Remote. Sens. **87**(2), 75–76 (2021)
7. Vecchi, E., Tavasci, L., Giorgini, E., Gandolfi, S.: A priori estimation of radar satellite interferometry's sensitivity for landslide monitoring in the Italian Emilia-Romagna region. Remote Sensing **16**(14), 2562 (2024)
8. De Montis, et al.: Integration of Geomatic, Geophysical and Chemical Data in a GIS Environment for Monitoring Contaminated Soils. In: International Conference on Computational Science and Its Applications, pp. 351–368. Springer Nature Switzerland, Cham (2024)
9. Bosco, C., Spano, D., Bacciu, V., Marras, S., Sirca, C.: Wildfire risk mapping and climate adaptation strategies in Mediterranean heritage areas. Sustainability **4**(10), 5987 (2022). https://doi.org/10.3390/su14105987
10. Bellomaria, G., Molfino, M.T., Fiorelli, M.: ArCo: The Italian cultural heritage knowledge graph. ArXiv (2019). https://arxiv.org/abs/1905.02840
11. UNIFI-IBAM-CNR. Risk maps for archaeological sites in southern Italy (2020)

12. Murgante, B., Borruso, G.: Geospatial technologies and climate change. Springer, Cham (2013)
13. Di Stefano, A., et al.: Wildfire risk in cultural landscapes: A case from central Italy. J. Cult. Herit. **48**, 141–151 (2021)
14. Cigna, F., et al.: The use of satellite data for risk assessment in cultural heritage. Remote Sensing **10**(8), 1226 (2018)
15. Olteanu, I., Crenganiș, L.M., Diac, M., Precul, A.M.: Sustainable approach of a multi-hazard risk assessment using GIS customized for Ungheni areal situated in the metropolitan area of Iasi. Sustainability **16**(11), 4485 (2024). https://doi.org/10.3390/su16114485
16. Bhunia, G.S., Shit, P.K.: Geospatial technology for multi-hazard risk assessment. In: Shit, P.K., Pourghasemi, H.R., Bhunia, G.S., Das, P., Narsimha, A. (eds.) Geospatial Technology for Environmental Hazards. Advances in Geographic Information Science. Springer, Cham (2022). https://doi.org/10.1007/978-3-030-75197-5_1
17. Shah, F.H., Ali, A., Iqbal, M.M.: A review on hazard risk assessment using remote sensing and GIS. Journal Central Asian Scientific Press **5**, 252–261 (2020)
18. SardegnArcheologica. "About.", https://www.sardegnarcheologica.it/text/1000/en. Last accessed 01 March 2025
19. Nurnet Geoportal. Nurnet Geoportal, n.d., https://nurnet.crs4.it/nurnetgeo/. Last accessed 01 March 2025
20. Regione Autonoma della Sardegna. Sardegna GeoNetwork, https://webgis2.regione.sardegna.it/geonetwork/srv/eng/catalog.search#/metadata/R_SARDEG:7a2ce3e7-2686-4c10-8df9-3a3c0ad013f2. Last accessed 01 March 2025
21. Regione Autonoma della Sardegna. Piano Stralcio di Bacino per l'Assetto Idrogeologico (PAI). 2006, https://autoritadibacino.regione.sardegna.it/pianificazione/piano-stralcio-di-bacino-per-lassetto-idrogeologico-pai/. Last accessed 01 March 2025
22. Regione Autonoma della Sardegna. Sardegna GeoNetwork, https://www.sardegnageoportale.it/webgis2/sardegnamappe/?map=pai. Last accessed 01 March 2025
23. Regione Autonoma della Sardegna, Direzione Generale della Protezione Civile. Carta del Pericolo Incendio Boschivo e di Interfaccia 2017. 2017, https://webgis2.regione.sardegna.it/geonetwork/srv/api/records/R_SARDEG:b3eff8cf-9cfc-497b-8423-3fc5a0749b51. Last accessed 01 March 2025
24. Salis, M., et al.: Analyzing seasonal patterns of wildfire exposure factors in Sardinia. Italy. Environmental Monitoring and Assessment **187**, 1–20 (2015)
25. Cardil, A., Salis, M., Spano, D., Delogu, G., Molina Terren, D.: Large wildland fires and extreme temperatures in Sardinia (Italy). iForest-Biogeosciences and Forestry **7**(3), 162 (2014)
26. Meletti, C., Camassi, R., Castelli, V.: A reappraisal of the seismicity of Sardinia. Italy. Seismological Society of America **92**(2A), 1148–1158 (2021)
27. Gorshkov, A., et al.: On the seismic potential of the Corsica-Sardinia block. Rendiconti Lincei. Scienze Fisiche e Naturali **32**, 715–728 (2021)
28. Anselmi, M., et al.: Microseismic assessment and fault characterization at the Sulcis (South-Western Sardinia) field laboratory. Int. J. Greenhouse Gas Control **95**, 102974 (2020)
29. Intergovernmental Panel on Climate Change (IPCC). Climate Change 2014: Impacts, Adaptation, and Vulnerability (Fifth Assessment Report, AR5). Cambridge University Press (2014). https://www.ipcc.ch/report/ar5/
30. Crichton, D.: The risk triangle. In: Ingleton, J. (ed.) Natural disaster management, pp. 102–103. Tudor Rose, London (1999)
31. Martín-Raya, N., Díaz-Pacheco, J., López-Díez, A.: Multi-hazard risk assessment analysis in La Palma: an approach for risk mitigation. Geoenvironmental Disasters **11**(1), 33 (2024)
32. Kappes, M.S., Keiler, M., von Elverfeldt, K., et al.: Challenges of analyzing multi-hazard risk: a review. Nat. Hazards **64**, 1925–1958 (2012). https://doi.org/10.1007/s11069-012-0294-2